

A. V. Plyukhin

# Autonomous Brownian motor driven by nonadiabatic variation of internal parameters

Received: date / Accepted: date

**Abstract** We discuss an autonomous motor based on a Brownian particle driven from thermal equilibrium by periodic in time variation of the internal potential through which the particle interacts with molecules of the surrounding thermal bath. We demonstrate for such a motor the absence of a linear response regime: The average driving force and drift velocity are shown to be quadratic in both the frequency and amplitude of the variation. The adiabatic approximation (of an infinitely slow variation) and the leading correction to it (linear in the variation's frequency) both lead to zero drift and are insufficient to describe the motor's operation.

**Keywords** Brownian motors · active transport · linear response

**PACS** 05.40.-a · 05.10.Gg · 05.60.-k · 05.20.-y

## 1 Introduction

Consider a Brownian particle moving in one dimension and interacting with molecules from the left and right through microscopic potentials  $U_l$  and  $U_r$ , which are of different shapes and/or ranges. Contrary to uncultivated intuition (but in agreement with thermodynamics), in thermal equilibrium such intrinsic microscopic asymmetry does not cause a net drift of the particle: Although a molecule, say, from the right interacts with the particle via a stronger force than a symmetrically positioned molecule from the left, the average forces exerted on the two sides of the particle, calculated with the equilibrium Boltzmann distribution, have exactly the same magnitudes and completely compensate each other. On a deeper level, this cancellation is ensured by detailed balance symmetry [1] which may (or may not) be broken

---

Department of Mathematics, Saint Anselm College, Manchester, NH, USA  
E-mail: aplyukhin@anselm.edu

when the system is out of equilibrium. Now suppose that the particle is active in the sense that it is equipped with an internal mechanism which modulates the static potentials  $U_l$  and  $U_r$  in a periodic-in-time manner

$$U_\alpha(t) = \xi_\alpha(t) U_\alpha, \quad (1)$$

e.g. with harmonic modulation functions

$$\xi_\alpha(t) = 1 + a_\alpha \sin \omega_\alpha t \quad (2)$$

with amplitudes  $0 < a_\alpha < 1$ . Here and below the subscript  $\alpha = \{l, r\}$  refers to the left and right sides of the particle. Such modulation may result from periodic conformational changes of internal degrees of freedom, which are very common for variety of biological macromolecules like proteins, ribosomes, and viruses. Now when the particle is out of equilibrium, one may reasonably expect that the asymmetry of static potentials  $U_\alpha$ , and/or the modulation amplitude  $a_\alpha$  and frequencies  $\omega_\alpha$  may result in the particle acquiring a nonzero average velocity and serving as a Brownian motor. As for many other machines operating under non-equilibrium conditions, the explicit evaluation of the drift force and velocity is a non-trivial problem, and even the direction of the drift may be not easy to guess. There are also a number of peculiar aspects of this model that we believe make it worthy to discuss.

Unlike many mesoscopic machines driven from equilibrium by *external* means (e.g., due to a contact with thermal baths of different temperatures, periodically in space and time modulated temperature, external potential, light, etc.), our motor is autonomous and resists the thermalization by means of the *internal* mechanism. Among other types of autonomous motors studied in recent years are granular Brownian systems [2], chemically powered motors driven by asymmetric catalytic activity [3], and Brownian information machines [4]. An autonomous active motor with an internal anchoring mechanism was studied in [5].

Driven by the oscillation of a *microscopic* parameter(s), our motor cannot be described within empirical approaches, e.g. those based on the standard Langevin or Fokker-Planck equations with time dependent external parameters [6, 7] or modified with the energy depot (“negative friction”) terms [8]. Only a few microscopic models of rectified Brownian motion are presented so far in literature, and most of them concern the regime beyond the weak coupling to the thermal bath. In such cases, the Fokker-Planck [9, 10, 11, 12, 13, 14, 15] and Langevin [15, 16] equations involve additional terms (of higher orders in a weak coupling parameter), and must be supplemented with additional fluctuation-dissipation relations which cannot be established phenomenologically. In contrast, for the present model a systematic driving force will be shown to emerge already in the leading order in the weak coupling parameter. Still, an explicit expression of the driving force cannot be constructed empirically and requires a microscopic evaluation.

One interesting property of the model is the absence of the linear response regime with respect to the modulation frequencies  $\omega$  considered as a perturbation parameter. For low  $\omega$ , the driving force and drift velocity

depend on frequency as  $\omega^2$ . Neither the adiabatic approximation (asymptotically slow modulation), nor the leading perturbational correction to it are sufficient to account for directional motion of the particle. A similar behavior was found previously for Brownian ratchets driven by temperature oscillations [6, 7, 17]. Other systems driven from equilibrium by variation of external parameters may show also qualitatively different scenarios ranging from directional transport driven by adiabatically slow variations [19, 20] to the absence of net transport beyond the adiabatic regime [21, 22]. Whether such diversity can also be observed in the family of autonomous machines like ours is yet to be explored.

It might be relevant to note that the absence of the linear response regime was previously observed also for motors with non-varying parameters but driven by the coupling with two baths with non-equal temperatures [12, 13, 14]. In that case, the prediction that the drift velocity must be an even function of a perturbation parameter (the temperature difference) can be envisaged from simple symmetry arguments. No similar arguments are apparently available for the present model.

Another remarkable feature of the model, which also has counterparts among motors driven by variation of external parameters [17, 18], is a non-monotonic dependence and - for certain regimes - the sign reversal of the drift velocity as a function of  $\omega$  (see Fig. 3 below). However, for our model such behavior is probably of only academic interest since it occurs when the period of modulation  $\omega^{-1}$  is unrealistically short - of order or shorter than the collision time  $\tau$ . Since the latter is usually the shortest characteristic time, we shall restrict our theoretical discussion to the low frequency limit  $\omega\tau \ll 1$ . Numerical simulation will be used to confirm theoretical predictions and to extend the results beyond the low frequency domain.

## 2 Model and simulation

We consider a Brownian particle of mass  $M$  immersed in the thermal bath of temperature  $T$  comprised of ideal gas molecules of mass  $m \ll M$ . Velocities of molecules before collisions with the particle are distributed with the Maxwell distribution

$$f_M(v) = \frac{1}{\sqrt{2\pi} v_T} \exp \left\{ -\frac{1}{2} \left( \frac{v}{v_T} \right)^2 \right\}, \quad (3)$$

where  $v_T = \sqrt{k_B T/m}$  is a thermal (mean-squared) velocity of a molecule. The motion of the particle and molecules of the bath is assumed to be one-dimensional.

Dynamics of the particle's internal degrees of freedom, are governed by a certain internal built-in mechanism whose specific design is immaterial for our purposes. When this mechanism is turned off the particle is "passive", i.e. behaves as a conventional Brownian particle interacting with molecules of the bath with time-independent forces. In order to facilitate analytic calculations, we assume that in the passive regime the bath molecules, unless their energy is too high, interact with the particle with constant repulsive forces of a finite

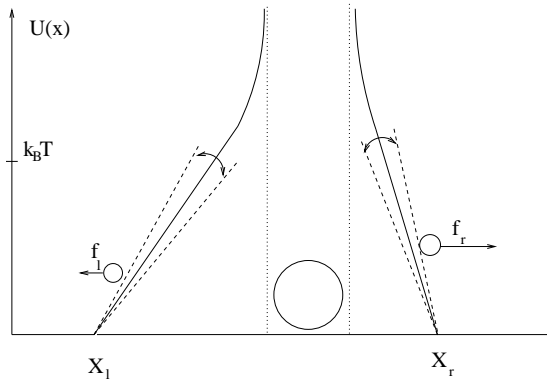


**Fig. 1** The solid line is the potential energy for the interaction of the motor (large circle) in the passive regime and a molecule of the bath (small circles) as a function of position of the latter. When a molecule is inside the left (right) interaction zone  $x > X_l$  ( $x < X_r$ ), it experiences a constant repulsive force of the amplitude  $f_l$  ( $f_r$ ). It is assumed that temperature is sufficiently low, so that only a negligible number of molecules with energy much higher than  $k_B T$  experience the upper nonlinear part of the potential. Dashed lines represent a periodic in time modulation of the potential for the active regime.

range, see Fig. 1. Namely, the potential energy of interaction of the particle with bath molecules on its left reads

$$U_l = f_l \sum_i (x_i - X_l) \theta(x_i - X_l). \quad (4)$$

Here  $x_i$  are coordinates of bath molecules,  $f_l$  is a positive constant of the force dimension,  $\theta(x)$  is the step-function. The coordinate  $X_l$  is associated with the left side of the particle and determines the boundary of the interaction zone for molecules coming from the left: molecules outside the interaction zone,  $x_i < X_l$ , do not interact with the particle, while every molecule inside the zone,  $x_i > X_l$ , exerts on the particle the same force  $f_l$ . Similarly, the potential energy of interaction with molecules on the right of the particles is

$$U_r = -f_r \sum_j (x_j - X_r) \theta(X_r - x_j), \quad (5)$$

where the positive constant  $f_r$  is the amplitude of the constant repulsive force exerted on the particle by a bath molecule from the right when the latter is in the right-hand side interaction zone,  $x_j < X_r$ .

To avoid complications related to the overlapping of left and right interaction zones, one can assume that closer to the particle's core the linear potential is replaced by a sharper (diverging) one, see Fig. 1. This, however, is of no consequence as soon as the crossover from the linear to nonlinear potentials occurs at the energy much higher than  $k_B T$ : only a negligible fraction of molecules with velocities  $v \gg v_T$  would feel the nonlinear part of the potential.

For this model the fluctuating Langevin force  $F(t)$  and its correlations can be readily evaluated analytically (see section 3 in [23]). To the lowest order

in the mass ratio parameter  $\lambda = \sqrt{m/M}$  and for the time scale much longer than the collision time (defined by Eq. (47) below) the Langevin equation for the particle's velocity  $V$  has the standard form

$$M \frac{dV}{dt} = -\gamma V + F(t). \quad (6)$$

A possible asymmetry of the microscopic forces,  $f_l \neq f_r$ , does not show up in this equation. Although the correlation function of the Langevin force  $\langle F(0)F(t) \rangle$  does depend on  $f_l$  and  $f_r$ , this dependence disappears after the integration over time. As a result, the damping coefficient  $\gamma$  does not depend on parameters of microscopic dynamics and takes the form

$$\gamma = \frac{1}{k_B T} \int_0^\infty \langle F(0)F(t) \rangle dt = 4\sqrt{\frac{2}{\pi}} n m v_T, \quad (7)$$

where  $n$  is the concentration of bath molecules. Also, if one writes  $F$  as a sum of forces on the left and right sides of the particle,  $F = F_l + F_r$ , one can show that

$$\langle F_l \rangle = -\langle F_r \rangle = n k_B T, \quad (8)$$

so the net Langevin force is zero-centered,  $\langle F(t) \rangle = 0$ . In accord with thermodynamics, the microscopic asymmetry does not bias equilibrium Brownian motion.

Our goal is to generalize the above microscopic model of passive Brownian motion for the case when the particle is "active", that is capable to vary the potentials  $U_l$  and  $U_r$  according to Eq. (1). For the active particle the potential energy of interaction with the bath is given by expressions similar to that for the passive regime

$$\begin{aligned} U_l(t) &= f_l(t) \sum_i (x_i - X_l) \theta(x_i - X_l) \\ U_r(t) &= -f_r(t) \sum_j (x_j - X_r) \theta(X_r - x_j), \end{aligned} \quad (9)$$

in which the static force magnitudes  $f_l$  and  $f_r$  are now replaced by time-dependent ones,

$$f_\alpha(t) = \xi_\alpha(t) f_\alpha, \quad (10)$$

where  $\xi_\alpha(t)$  is given by (2),  $\xi_\alpha(t) = 1 + a_\alpha \sin \omega_\alpha t$  (to minimize the number of parameters we assume no phase shift). Clearly, such a variation requires an external input of energy, which is not explicitly reflected in the model.

The modulation frequencies  $\omega_\alpha$  will be assumed to be small compared to the characteristic collision time, while the amplitudes  $a_\alpha$  are not necessarily small and may take any values from the interval  $(0, 1)$ . The values  $a_\alpha = 1$ , though not altogether meaningless (may correspond to a permeable particle, see [23]), are not considered. The variation of the particle-bath interaction supports the particle in a nonequilibrium state, which is the first condition of the drift. The second condition - the break of the spatio-temporal symmetry

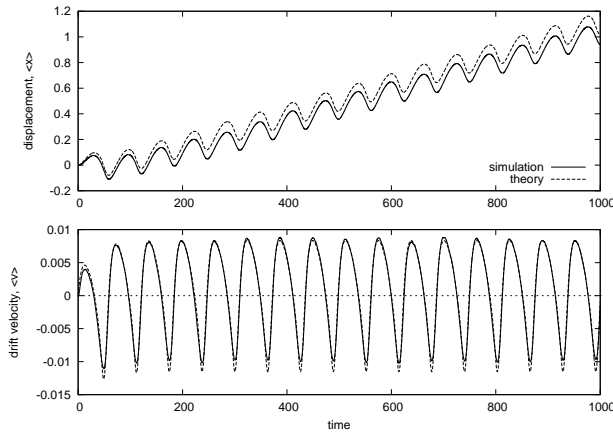


**Fig. 2** Average displacement  $\langle x(t) \rangle$  and velocity  $\langle v(t) \rangle$  of the motor as functions of time for regime (11) with parameters  $\omega_r = \omega_l = 0.1$ ,  $a_r = a_l = 0.5$ , and  $\delta = f_r/f_l = 3$ . Numerical experiment data (solid lines) are averaged over about  $2 \cdot 10^5$  trajectories. Theoretical curves (dashed lines) are solutions of the Langevin equation (56) which corresponds to the average fluctuating force  $\langle F(t) \rangle$  given by Eq. (54). Units are defined by Eqs. (55).

- can be arranged by assigning different sets of values  $\{f_\alpha, a_\alpha, \omega_\alpha\}$  for the left and right sides of the particle.

We study this model both theoretically and using numerical simulation. The latter is performed for the mass ratio  $\lambda^2 = m/M = 0.01$  with the standard molecular dynamics scheme with the only difference that instead of using periodic boundary conditions, we generate in the beginning of each simulation run a very large thermal bath of noninteracting molecules (see [23] for details). The simulation shows that for unequal sets  $\{f_l, a_l, \omega_l\}$  and  $\{f_r, a_r, \omega_r\}$  the particle develops non-stationary drift velocity, whose direction and value depend on  $f_\alpha, a_\alpha, \omega_\alpha$  in a rather subtle way.

As a showcase example let us consider the case when asymmetry is due to non-equal magnitudes of the static (passive) forces,  $f_l \neq f_r$ . Specifically, suppose that the particle, while in the passive regime, interacts with a molecule on the right via a stronger static force than with a molecule from the left (as in Fig. 1), while the modulation parameters for the left and right sides are the same,

$$f_l < f_r, \quad \omega_l = \omega_r = \omega, \quad a_l = a_r = a. \quad (11)$$

For this case, when the modulation frequency is sufficiently low, the simulation shows that the particle drifts to the right, that is in the direction of the steeper slope of the internal potential, see Fig. 2. Perhaps somewhat counter-intuitive, this behavior is in agreement with a theory which will be developed in sections to follow. Note that for the given values of parameters the drift is rather small and becomes visible only after taking average over many particle's trajectories. A single trajectory looks like a random path of a passive Brownian particle and shows no visible bias. All experimental curves in this paper represent data averaged over about  $10^5$  trajectories.

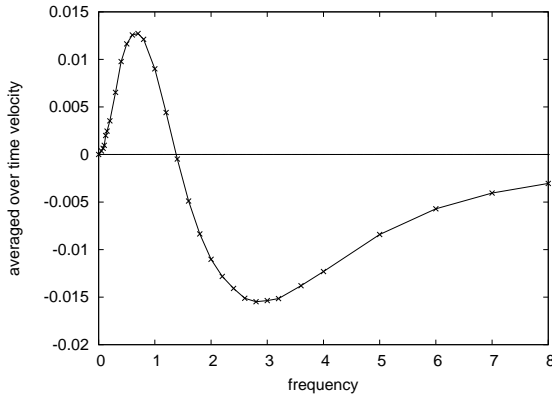


**Fig. 3** Drift velocity of the motor averaged over time as a function of the modulation frequency  $\omega$  for regime (11) with parameters  $a_r = a_l = 0.5$ , and  $\delta = f_r/f_l = 3$ . Each experimental point corresponds to an ensemble-averaged trajectory similar to that in Fig. 2.

Another interesting feature suggested by simulation data is that for low  $\omega$  the drift velocity increases with frequency as  $\omega^2$ . This can be interpreted as the absence of the linear response regime with respect to  $\omega$  as a perturbation. As frequency is getting higher, the frequency dependence of the drift velocity becomes nonmonotonic, and the inversion of the drift direction occurs, see Fig. 3.

According to (10), molecules in the left and right interaction zones of the motor experience the forces of magnitudes

$$f_\alpha(t) = f_\alpha + f_\alpha a_\alpha \sin \omega_\alpha t. \quad (12)$$

One observes that for the regime defined by Eq. (11) both static and time-dependent parts of these expressions are different for the left and right sides of the particle. It is natural to ask if the drift still occurs when asymmetry affects only the static parts,

$$f_l < f_r \quad f_l a_l = f_r a_r, \quad \omega_l = \omega_r. \quad (13)$$

or only dynamic parts, e.g.

$$f_l = f_r \quad a_l < a_r, \quad \omega_l = \omega_r. \quad (14)$$

The simulation shows the drift in both these cases too, but with no sign reversal and in opposite directions, see Fig. 4. This suggests that the reversal of the drift direction for regime (11) can be interpreted as a result of the interplay or interference of two regimes described by Eqs. (13) and (14).

Another interesting regime of the motor's operation is when the drift is induced by unequal modulation frequencies (one frequency may be zero), while the pair of other parameters is the same for both sides of the particle,

$$f_l = f_r \quad a_l = a_r, \quad \omega_l \neq \omega_r. \quad (15)$$

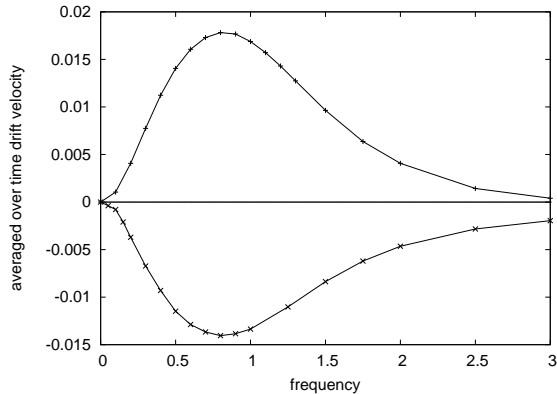


**Fig. 4** Drift velocity of the motor averaged over time as a function of the modulation frequency  $\omega$ . The upper curve corresponds to the regime (13) (asymmetric static part of interaction) with  $f_r/f_l = 3$  and  $f_l a_l = f_r a_l = 0.5$ . The bottom curve is for regime (14) (asymmetric dynamical part of interaction) with  $a_r = 0.25$  and  $a_l = 0.5$ .

In this case, if one or both frequencies are low (much shorter than the collision time), the particle drifts in the direction of the side with lower modulation frequency (two upper curves in Fig. 5). On the other hand, if both frequencies are high, the particle systematically moves in the direction of the side with a higher frequency (a bottom curve in Fig. 5).

In the following sections we shall focus on a theoretical description of the model. We shall not try to cover the whole rich phenomenology which the model shows in simulation, but rather restrict ourselves to developing a perturbation approach for the low frequency domain.

### 3 Theory: basic relations

We assume that in the active regime the particle is still described by the Langevin equation (6) with the damping coefficient approximately the same as for the passive regime, i.e. given by (7), but with a non-zero centered fluctuating force,  $\langle F(t) \rangle \neq 0$ . The goal is to evaluate microscopically  $\langle F(t) \rangle$  and then, solving the averaged Langevin equation

$$M \frac{d}{dt} \langle V(t) \rangle = -\gamma \langle V(t) \rangle + \langle F(t) \rangle, \quad (16)$$

find the average velocity  $\langle V(t) \rangle$  and trajectory  $\langle X(t) \rangle$  of the motor.

An obvious drawback of this approach is that it neglects the influence of the active part of the fluctuating force  $F(t)$  on the damping coefficient  $\gamma$ . Since the two quantities are related by a fluctuation-dissipation relation, this approximation cannot be entirely consistent. Yet it is clear that for sufficiently small  $\omega_\alpha$  or/and  $a_\alpha$  an “active” correction to the dissipation constant is small compared to the value of the latter for the passive regime, and thus

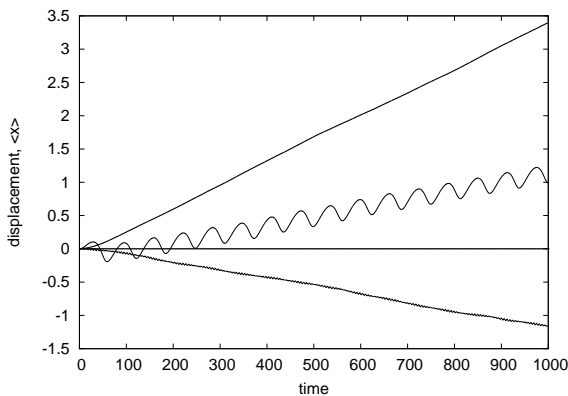


**Fig. 5** Average displacement  $\langle x(t) \rangle$  of the motor as a function of time for regime (15) when asymmetry is due to unequal modulation frequency,  $\omega_l \neq \omega_r$ . The upper line is for  $\omega_l = 2.5$  and  $\omega_r = 0$ , the middle line is for  $\omega_l = 0.1$  and  $\omega_r = 0$ , and the bottom line is for  $\omega_l = 1.1$  and  $\omega_r = 1$ . For all lines the modulations amplitudes are the same  $a_l = a_r = 0.5$ . The oscillatory character of the upper line is imperceptible on the figure's scale.

should produce a little effect. We shall see that the comparison of the theory with simulation results supports this intuition.

As known from the microscopic theory of Brownian motion, the Langevin equation (6) corresponds to the lowest order approximation in the mass ratio  $m/M$ , in which case the fluctuating force  $F(t)$  can be evaluated neglecting the particle's motion. Setting  $F = F_l + F_r$ , let us consider the force  $F_l$  exerted on the particle, fixed in space, by molecules coming from the left. For the linear potential (9), each molecule in the left interaction zone  $x > X_L$  exerts on the particle the same time dependent force  $f_l(t)$ . Then the total force on the left side is given simply by the product

$$F_l(t) = f_l(t) N_l(t), \quad (17)$$

where the  $N_l(t)$  is the number of molecules in the left interaction zone at a given time,

$$N_l(t) = \int_{-\infty}^{\infty} dv \int_{X_l}^{\infty} dx f(x, v, t). \quad (18)$$

Here  $f(x, v, t) = \sum_i \delta(x - x_i) \delta(v - v_i)$  is the microscopic density of molecules in the position and velocity space. For simplicity we extended the right border of the left interaction zone to infinity. For low enough temperature the effect of such approximation is negligible.

It is convenient to define the collision time  $\tau_l(v, t)$  as a time spent in the interaction zone  $x > X_l$  by a molecule which enters the zone with velocity  $v$  and leaves the zone at time  $t$ . The collision time  $\tau_r(v, t)$  for molecules hitting the particle's right side is defined in a similar way. The dependence of  $\tau_\alpha(v, t)$  on time reflects the dynamical nature of the interaction potentials (9).

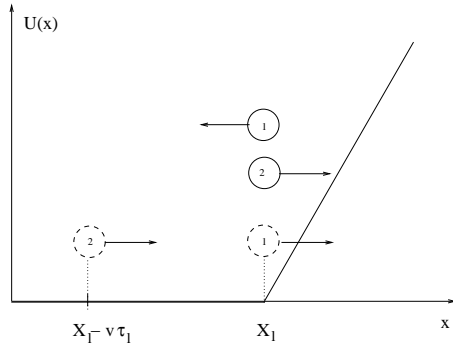


**Fig. 6** Solid line circles: at time  $t$  molecule two is just before the collision entering the left interaction zone  $x > X_l$ , and molecules one is just after the collision leaving the interaction zone. Dashed line circles show same molecules at time  $t - \tau_l$ .

Of course, for the passive regime the collision times depends on molecule's pre-collision velocity only.

Consider two molecules with the same pre-collision velocity  $v > 0$  at the border of the interaction zone  $X_L$  at time  $t$ . Molecule one is just after the collision, departing the interaction zone,

$$x_1(t) = X_l, \quad v_1(t) < 0, \quad (19)$$

while molecule two is just before the collision, entering the interaction zone,

$$x_2(t) = X_l, \quad v_2(t) = v > 0, \quad (20)$$

see Fig. 6. According to the definition of  $\tau_\alpha(v, t)$ , at earlier time  $t - \tau_l(v, t)$  both molecules had velocity  $v > 0$  and coordinates

$$x_1(t - \tau_l) = X_l, \quad x_2(t - \tau_l) = X_l - v \tau_l. \quad (21)$$

For the low modulation frequency it is reasonable to assume that molecules with the same initial velocity do not bypass each other in the interaction zone. Then it is clear that *all* molecules with a pre-collision velocity  $v > 0$  which are in the interaction zone at time  $t$ , at the time  $t - \tau_l$  were within the interval

$$[x_1(t - \tau_l), x_2(t - \tau_l)] = [X_l - v \tau_l, X_l] \quad (22)$$

and moving to the right with velocity  $v$ , see Fig. 6. Thus for the number of molecules in the interaction zone at a given time, instead of (18) one can write

$$N_l(t) = \int_0^\infty dv \int_{X_l - v \tau_l}^{X_l} dx f(x, v, t - \tau_l). \quad (23)$$

The advantage of this form is that it involves integration over coordinates and velocities of molecules before collisions with the particle, in which case

the microscopic density is simply the Maxwell distribution  $f_M(v)$  multiplied by the average concentration of bath molecules  $n$ ,

$$\langle f(x, v, t) \rangle = n f_M(v). \quad (24)$$

Then from (23) for the average number of molecules in the interaction zone one obtains

$$\langle N_l(t) \rangle = n \int_0^\infty dv f_M(v) v \tau_l(v, t), \quad (25)$$

and the average force on the left side of the particle  $\langle F_l(t) \rangle = f_l(t) \langle N_l(t) \rangle$  takes the form

$$\langle F_l(t) \rangle = n f_l(t) \int_0^\infty dv f_M(v) v \tau_l(v, t). \quad (26)$$

Similarly, the average force on the right side of the particle is

$$\langle F_r(t) \rangle = -n f_r(t) \int_{-\infty}^0 dv f_M(v) v \tau_r(v, t). \quad (27)$$

To advance further, we need to evaluate collision times  $\tau_\alpha(v, t)$  for the active regime, which will be the focus of the next section. Meanwhile, it is instructive to consider how the general expressions (26) and (27) work for the passive regime, when  $f_\alpha(t) = f_\alpha = \text{const}$ . In this case the collision times do not depend on time and we shall denote them as  $\tau_\alpha^0(v)$ . Consider a molecule which enters, say, the left interaction zone at the moment  $t = 0$  with the initial velocity  $v > 0$ . While the molecule is still in the zone its velocity evolves as

$$v(t) = v - \frac{f_l}{m} t. \quad (28)$$

The collision time  $\tau_l^0$  corresponds to the moment when the molecule leaves the zone with velocity  $-v$ . The equation  $v(\tau_l^0) = -v$  gives

$$\tau_l^0(v) = \frac{2mv}{f_l}. \quad (29)$$

Similarly, the right side collision time is

$$\tau_r^0(v) = \frac{2mv}{f_r}. \quad (30)$$

Substitution of these expression into Eqs.(26) and (27) gives the result (8) of the elementary kinetic theory

$$\langle F_l \rangle = -\langle F_r \rangle \equiv F_0 = n m \langle v^2 \rangle = n k_B T. \quad (31)$$

As expected, for the passive regime the asymmetry  $f_l \neq f_r$  does not induce a net driving force on the particle. We can now interpret this no-go result as follows: Each molecule in the  $\alpha$ -th interaction zone pushes the particle with a force of magnitude  $f_\alpha$ , but the average zone's population  $\langle N_\alpha \rangle$ , according to (25), is linear in the collision time  $\tau_\alpha$ , which in turn is inversely proportional to  $f_\alpha$ ,  $\tau_\alpha \sim 1/f_\alpha$ . As a result, for the average force  $\langle F_\alpha \rangle \sim f_\alpha \langle N_\alpha \rangle$  the dependence on  $f_\alpha$  is canceled out.

#### 4 Collision time for active regime

Above we defined the collision time  $\tau_\alpha(v, t)$  as functions of the pre-collision velocity  $v$  and after-collision exit time  $t$ , which corresponds to the moment when a molecule is *leaving* the interaction zone. With these functions one can express the forces  $\langle F_\alpha(t) \rangle$  on two particle's sides in simple forms (26) and (27). The disadvantage of functions  $\tau_\alpha(v, t)$  is that they are difficult to evaluate directly. Let us define collision times  $\tau_\alpha^*(v, t)$  whose first argument is still velocity before the collision, while the time argument refers now to the moment when a molecule *enters* the interaction zone. Since both arguments of  $\tau_\alpha^*(v, t)$  refer to the same pre-collision moment, these functions are easier to evaluate. The two functions  $\tau_\alpha(v, t)$  and  $\tau_\alpha^*(v, t)$  are related by the equation

$$\tau(t) = \tau^*(t - \tau(t)). \quad (32)$$

Here and for the bulk of this section we omit for brevity the argument  $v$  which is assumed to be the same for all quantities, and also suppress the left/right index  $\alpha$ . We shall restore  $\alpha$  in the final expression for  $\tau_\alpha$ .

In order to find an explicit expression for  $\tau$  in terms of  $\tau^*$  we approximate the right hand side of Eq. (32) by the first three terms of the Taylor expansion about  $t$ ,

$$\tau \approx \tau^* - (\tau^*)' \tau + \frac{1}{2} (\tau^*)'' \tau^2, \quad (33)$$

where primes denote time derivatives. Since  $(\tau^*)' \sim \omega$  and  $(\tau^*)'' \sim \omega^2$ , the above relation is of second order in  $\omega$ . To the same order, the solution of Eq. (33) has a form

$$\tau = \tau^* - (\tau^*)' \tau^* + \frac{1}{2} (\tau^*)'' (\tau^*)^2 + [(\tau^*)']^2 \tau^*, \quad (34)$$

which produces a desirable explicit expression of  $\tau$  in terms of  $\tau^*$ . Our goal now is first to evaluate  $\tau^*$ , and then using (34) to find  $\tau$ . Substitution of  $\tau$  into Eqs. (26) and (27) will give us a perturbation expression for the force on the particle to second order in  $\omega$ .

Consider a molecule which enters the left interaction zone  $x > X_l$  with velocity  $v_0 > 0$  at the moment  $t = t_0$ . Setting for a moment  $X_l = 0$ , the equation of motion and initial conditions read

$$\begin{aligned} m x''(t) &= -f(t) = -f \xi(t) \\ x(t_0) &= 0, \quad x'(t_0) = v_0, \end{aligned} \quad (35)$$

where  $\xi(t)$  is given by (2). The solution of the initial value problem (35) is convenient to write as a function of time  $t$  elapsed since the moment  $t_0$  when the molecule enters the zone:

$$\begin{aligned} x(t) &= v_0 t - \frac{f}{2m} t^2 + \\ &\frac{f a}{m \omega^2} \left( \sin \omega(t_0 + t) - \sin \omega t_0 - \omega t \cos \omega t_0 \right). \end{aligned} \quad (36)$$

Recall that for the passive regime, the collision time  $\tau^*$  can be determined from the equation  $v(\tau^*) = -v$ , since the speed of a molecule before and after the collision is the same. That is, of course, not so for a time-dependent potential. For the active regime the collision time  $\tau^*(v_0, t_0)$  should be found as a nonzero solution of the equation

$$x(\tau^*) = 0. \quad (37)$$

We wish to find an approximate solution of this equation to order  $\omega^2$  (an appropriate dimensionless small parameter is introduced by equation (49) below). Using in (36) the truncated expansion

$$\begin{aligned} \sin \omega(t_0 + t) &\approx \sin \omega t_0 + \cos \omega t_0 (\omega t) - \frac{1}{2} \sin \omega t_0 (\omega t)^2 \\ &- \frac{1}{6} \cos \omega t_0 (\omega t)^3 + \frac{1}{24} \sin \omega t_0 (\omega t)^4, \end{aligned} \quad (38)$$

one obtains to order  $\omega^2$

$$x(t) = x_{ad}(t) - \frac{f a \omega \cos \omega t_0}{6 m} t^3 + \frac{f a \omega^2 \sin \omega t_0}{24 m} t^4. \quad (39)$$

Here the first term is of zero order in  $\omega$

$$x_{ad}(t) = v_0 t - \frac{f(t_0)}{2m} t^2, \quad (40)$$

and corresponds to the adiabatic approximation which completely neglects the change of the potential during the collision. As we shall see below, the adiabatic approximation  $x(t) \approx x_{ad}(t)$  is not sufficient to account for the motor's drift. The two last terms in (39) are of first and second order in  $\omega$ , and take into account the dynamical nature of the potential.

Substitution of (39) into (37) and resetting  $(v_0, t_0) \rightarrow (v, t)$  gives for the collision time  $\tau^*(v, t)$  a cubic algebraic equation which we write in the following dimensionless form:

$$\xi(t) \left( \frac{\tau^*}{\tau^0} \right) + \frac{1}{3} a (\omega \tau^0) \cos \omega t \left( \frac{\tau^*}{\tau^0} \right)^2 - \frac{1}{12} a (\omega \tau^0)^2 \sin \omega t \left( \frac{\tau^*}{\tau^0} \right)^3 = 1, \quad (41)$$

where, recall,  $\tau^0 = \tau^0(v) = 2mv/f$  is the collision time for the passive regime. Solving this equation perturbatively to order  $\omega^2$ , one obtains (see Appendix):

$$\begin{aligned} \tau^* &= \tau^0 \left\{ \xi^{-1}(t) - \frac{a}{3} (\omega \tau^0) \xi^{-3}(t) \cos \omega t \right. \\ &\left. + \frac{a}{12} (\omega \tau^0)^2 \xi^{-4}(t) \sin \omega t + \frac{2a^2}{9} (\omega \tau^0)^2 \xi^{-5}(t) \cos^2 \omega t \right\}. \end{aligned} \quad (42)$$

Recall that  $\tau^*(v, t)$  is a function of a time when a molecule enters the interaction zone, while the expressions (26) and (27) for the average forces involves the collision time  $\tau(v, t)$  as a function of the time when a molecule leaves the zone. To second order in  $\omega$  the relation between  $\tau^*$  and  $\tau$  is given

by Eq. (34). Substituting (42) into (34), neglecting terms of order higher than  $\omega^2$ , and restoring the right/left index  $\alpha$  we obtain

$$\begin{aligned} \tau_\alpha = \tau_\alpha^0 \left\{ \xi_\alpha^{-1}(t) + \frac{2a_\alpha}{3} (\omega_\alpha \tau_\alpha^0) \xi_\alpha^{-3}(t) \cos \omega_\alpha t \right. \\ \left. + \frac{a_\alpha}{4} (\omega_\alpha \tau_\alpha^0)^2 \xi_\alpha^{-4}(t) \sin \omega_\alpha t + \frac{8a_\alpha^2}{9} (\omega_\alpha \tau_\alpha^0)^2 \xi_\alpha^{-5}(t) \cos^2 \omega_\alpha t \right\}. \end{aligned} \quad (43)$$

To zeroth order in  $\omega$  this expression gives

$$\tau_\alpha(v, t) \approx \tau_\alpha^0(v) \xi_\alpha^{-1}(t) = \frac{2mv}{f_\alpha(t)}. \quad (44)$$

This is just the expression for the collision time  $\tau_\alpha^0$  for the passive regime, given Eqs. (29) and (30), in which the static force magnitudes  $f_\alpha$  are replaced by dynamic ones  $f_\alpha(t) = f_\alpha \xi_\alpha(t)$ . Thus the expression (44) corresponds to the adiabatic approximation and, as one can check, can be derived as a solution of the equation  $x_{ad}(\tau^*) = 0$  with  $x_{ad}(t)$  given by (40).

Three last terms in the right hand side of Eq. (43) describe corrections to the adiabatic approximation up to order  $\omega^2$ . These terms behave differently being time-averaged over the period of modulation: the term linear in  $\omega$  vanishes, whereas the terms quadratic in  $\omega$  do not vanish and have opposite signs. As we shall see in the next section, it is these two last terms which are responsible for the particle's drift.

## 5 Driving force

Substitution of Eq. (43) for the collision times into Eqs. (26) and (27) yields the following expression for the average forces on two sides of the particle:

$$\begin{aligned} \langle F_\alpha(t) \rangle = \pm F_0 \left\{ 1 + c_1 (\omega_\alpha \hat{\tau}_\alpha) a_\alpha \xi_\alpha^{-2}(t) \cos \omega_\alpha t \right. \\ \left. + c_2 (\omega_\alpha \hat{\tau}_\alpha)^2 a_\alpha \xi_\alpha^{-3}(t) \sin \omega_\alpha t + c_3 (\omega_\alpha \hat{\tau}_\alpha)^2 a_\alpha^2 \xi_\alpha^{-4}(t) \cos^2 \omega_\alpha t \right\}. \end{aligned} \quad (45)$$

Here the sign of the right hand side is plus and minus respectively for the force on the left ( $\alpha = l$ ) and right ( $\alpha = r$ ) sides of the particle,  $F_0$  is the magnitude of the force on each side for the passive regime given by (31),

$$F_0 = nk_B T = n m v_T^2, \quad (46)$$

$\hat{\tau}_\alpha$  is the collision time for the passive regime for a molecule with the thermal speed  $v_T = \sqrt{k_B T/m}$ ,

$$\hat{\tau}_\alpha = \tau_\alpha^0(v_T) = \frac{2 m v_T}{f_\alpha}, \quad (47)$$

and numerical coefficients are

$$c_1 = \frac{4}{3} \sqrt{\frac{2}{\pi}}, \quad c_2 = \frac{3}{4}, \quad c_3 = \frac{8}{3}. \quad (48)$$

The above expression (45) is a perturbation expansion of the average force up to second order in  $\omega$ , or more precisely, in the dimensionless parameter

$$\epsilon_\alpha = \omega_\alpha \hat{\tau}_\alpha. \quad (49)$$

The approximation of zeroth order  $\langle F_\alpha(t) \rangle \approx \pm F_0$  coincides with the force for the passive regime, Eq. (31), and corresponds to the adiabatic approximation (44) for the collision time which neglects the variation of the potential during the collision. As expected, in the adiabatic approximation, asymmetry of the static force magnitudes  $f_\alpha$  and of parameters of dynamic modulation  $(a_\alpha, \omega_\alpha)$  do not show up, and the the total average force on the particle  $\langle F \rangle = \langle F_l \rangle + \langle F_r \rangle$  is zero.

The lowest order correction to the adiabatic approximation in linear in  $\omega_\alpha$  (or  $\epsilon_\alpha$ ) and is presented by the second term in the right hand side of Eq.(45). If one considers  $\omega$  as a variable responsible for perturbation from equilibrium, the truncation

$$\langle F_\alpha(t) \rangle \approx \pm F_0 \left\{ 1 + c_1 (\omega_\alpha \hat{\tau}_\alpha) a_\alpha \xi_\alpha^{-2}(t) \cos \omega_\alpha t \right\} \quad (50)$$

can be interpreted as a linear response approximation. In contrast to the adiabatic approximation, asymmetry of static and dynamic parameters is manifestly present here, and the time-dependent part of the total average force  $\langle F \rangle = \langle F_l \rangle + \langle F_r \rangle$  does not vanish. However, if in addition to the ensemble average one also evaluates the time average over the period of modulation, the function  $\xi_\alpha^{-2}(t) \cos \omega_\alpha t$  vanishes, and so do the total average force and the average velocity of the particle. The absence of the drift in this case can also be directly demonstrated solving the Langevin equation (16). Thus the linear response approximation (50) is insufficient to account for the operation of the system as a motor.

The last two terms in the right hand side of Eq. (45) are of second order in  $\omega_\alpha$  and present the correction to the linear respond approximation. Both terms do not vanish under time averaging over the modulation period and thus can generate a drift of the particle. As one can check, the time averages of these two terms are of opposite signs.

We finish this section with a remark that our derivation of Eq. (45) for the average forces does not assume that the modulation amplitudes  $a_\alpha$  are small. An additional assumption  $a_\alpha \ll 1$  and the linear approximation for the functions  $\xi_\alpha^{-n}(t)$

$$\xi_\alpha^{-n}(t) \approx 1 - a_\alpha n \sin \omega_\alpha t \quad (51)$$

bring Eq. (45) to order  $a_\alpha^2$  to the following form

$$\begin{aligned} \langle F_\alpha(t) \rangle = \pm F_0 \left\{ 1 + c_1 (\omega_\alpha \hat{\tau}_\alpha) a_\alpha \cos \omega_\alpha t - c_1 (\omega_\alpha \hat{\tau}_\alpha) a_\alpha^2 \sin 2 \omega_\alpha t \right. \\ \left. + c_2 (\omega_\alpha \hat{\tau}_\alpha)^2 a_\alpha \sin \omega_\alpha t + (\omega_\alpha \hat{\tau}_\alpha)^2 a_\alpha^2 [c_3 \cos^2 \omega_\alpha t - 3 c_2 \sin^2 \omega_\alpha t] \right\}. \end{aligned}$$

Clearly, only the last term, quadratic in both  $\omega_\alpha$  and  $a_\alpha$ , contributes to the drift of the motor. Thus for the present model the drift is a nonlinear phenomenon with respect to both modulation parameters.

When both  $\omega_\alpha$  and  $a_\alpha$  are small the drift is small too and numerical simulation becomes very time-consuming. In remaining sections we shall work with the more general expression (45) which does not assume the smallness of  $a_\alpha$ .

## 6 Results

In this section we discuss solutions of the Langevin equation (16) with the average fluctuating force given by Eq. (45). Although the equation is linear, its explicit analytic solutions are rather bulky and not instructive. We therefore present solutions in a graphical form only.

Let us first consider the case already discussed in Section II when the asymmetry is due to unequal magnitudes of the passive forces  $f_l \neq f_r$ , while the modulation frequencies and amplitudes for the left and right sides are the same,

$$\omega_l = \omega_r = \omega, \quad a_l = a_r = a, \quad \xi_l(t) = \xi_r(t) = \xi(t). \quad (52)$$

Introducing the parameter of asymmetry  $\delta$  by relations

$$f_r = \delta f_l, \quad \text{or} \quad \hat{\tau}_r = \delta^{-1} \hat{\tau}_l, \quad (53)$$

one obtains from (45) the following expression for the total average force  $\langle F \rangle = \langle F_l \rangle + \langle F_r \rangle$ :

$$\begin{aligned} \langle F(t) \rangle = F_0 \bigg\{ & c_1 (\omega \hat{\tau}_l) (1 - \delta^{-1}) a \xi^{-2}(t) \cos \omega t \\ & + c_2 (\omega \hat{\tau}_l)^2 (1 - \delta^{-2}) a \xi^{-3}(t) \sin \omega t \\ & + c_3 (\omega \hat{\tau}_l)^2 (1 - \delta^{-2}) a^2 \xi^{-4}(t) \cos^2 \omega t \bigg\}. \end{aligned} \quad (54)$$

This expression is to be substituted into the Langevin equation (16), which we integrate numerically using the following time, space, and velocity units

$$t_0 = \frac{1}{2} \hat{\tau}_l = \frac{mv_T}{f_l}, \quad x_0 = v_T t_0, \quad v_0 = \frac{x_0}{t_0} = v_T. \quad (55)$$

The same units of course are employed in simulation. (Note that the acceleration unit is  $a_0 = v_0/t_0 = f_l/m$ , which means that molecules in the left interaction zone have acceleration of magnitude one).

In dimensionless form the Langevin equation (16) with the force (54) and  $\gamma$  given by (7) reads as follows

$$\begin{aligned} \frac{d}{d\tilde{t}} \langle \tilde{V} \rangle = & -3 c_1 \lambda^2 \tilde{n} \langle \tilde{V} \rangle + 2 c_1 \lambda^2 \tilde{n} a \tilde{\omega} (1 - \delta^{-1}) \xi^{-2}(t) \cos \tilde{\omega} \tilde{t} \\ & + 4 c_2 \lambda^2 \tilde{n} a \tilde{\omega}^2 (1 - \delta^{-2}) \xi^{-3}(t) \sin \tilde{\omega} \tilde{t} \\ & + 4 c_3 \lambda^2 \tilde{n} a^2 \tilde{\omega}^2 (1 - \delta^{-2}) \xi^{-4}(t) \cos^2 \tilde{\omega} \tilde{t}, \end{aligned} \quad (56)$$

where  $\lambda = \sqrt{m/M}$ , and a superposed tilde is used to denote dimensionless velocity  $\tilde{V} = V/v_0$ , time  $\tilde{t} = t/t_0$ , frequency  $\tilde{\omega} = \omega t_0$ , and the concentration

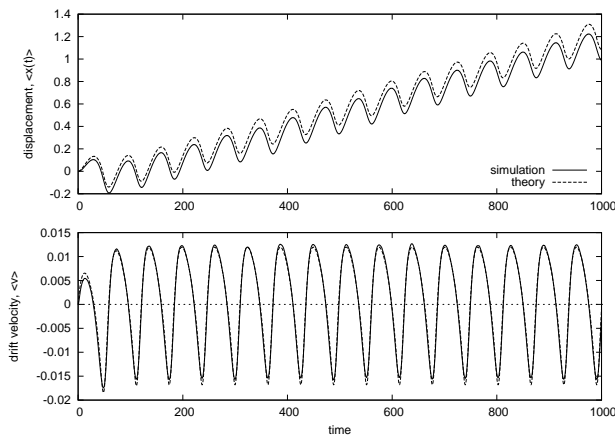


**Fig. 7** Average displacement  $\langle x(t) \rangle$  and velocity  $\langle v(t) \rangle$  of the motor as functions of time for regime (57) with parameters  $\omega = 0.1$ ,  $a = 0.5$ , and  $f_r = f_l = 1$ . Simulation data (solid lines) are averaged over about  $2 \cdot 10^5$  trajectories. Theoretical curves (dashed lines) are solutions of the Langevin equation (59).

of bath molecules  $\tilde{n} = n x_0$ . Since the operations of taking a time derivative  $d/dt$  and an ensemble average  $\langle \dots \rangle$  clearly commute, the equation for the dimensionless displacement  $\tilde{X} = X/x_0$  follows from (56) simply by the replacement  $\langle \tilde{V} \rangle = \frac{d}{dt} \langle \tilde{X} \rangle$ . The solutions for  $\langle \tilde{X}(\tilde{t}) \rangle$  and  $\langle \tilde{V}(\tilde{t}) \rangle$  are presented in Fig. 2 for zero initial conditions by dashed lines. They are in good agreement with numerical simulation (solid lines) provided the modulation amplitude is not too high,  $a \leq 0.5$ .

Motors with other types of asymmetry can be considered in similar ways. As another example, let us compare predictions of the theory and simulation results for the case when the left side of the particle is active, while the right side is passive,

$$\omega_l = \omega \neq 0, \quad a_l = a \neq 0 \quad \omega_r = a_r = 0. \quad (57)$$

For this case, the general expression (45) gives the following result for the ensemble-average fluctuating force on the particle

$$\langle F(t) \rangle = F_0 \left\{ c_1 (\omega \hat{\tau}) a \xi^{-2}(t) \cos \omega t \right. \\ \left. + c_2 (\omega \hat{\tau})^2 a \xi^{-3}(t) \sin \omega t + c_3 (\omega \hat{\tau})^2 a^2 \xi^{-4}(t) \cos^2 \omega t \right\}, \quad (58)$$

where all quantities are for the particle's left side. The corresponding Langevin equation for the average velocity in dimensionless notations has the form

$$\frac{d}{dt} \langle \tilde{V} \rangle = -3 c_1 \lambda^2 \tilde{n} \langle \tilde{V} \rangle + 2 c_1 \lambda^2 \tilde{n} a \tilde{\omega} \xi^{-2}(t) \cos \tilde{\omega} \tilde{t} \\ + 4 c_2 \lambda^2 \tilde{n} a \tilde{\omega}^2 \xi^{-3}(t) \sin \tilde{\omega} \tilde{t} + 4 c_3 \lambda^2 \tilde{n} a^2 \tilde{\omega}^2 \xi^{-4}(t) \cos^2 \tilde{\omega} \tilde{t}. \quad (59)$$

The solution of this equation and of a similar equation for the dimensionless displacement  $\langle \tilde{X}(\tilde{t}) \rangle$  are presented by dashed lines in Fig. 7. Again,

within the range of its validity,  $\omega\tau \ll 1$ , the theory agrees with simulation provided  $a \leq 0.5$ . As the variation amplitude  $a$  is further increased, the theory progressively overestimates the drift velocity. We believe this is due to neglected effects of the variation on the dissipative force in the Langevin equation. A small offset between theoretical and experimental curves visible in both Fig. 2 and Fig. 7 can probably be attributed to non-Markovian effects which are also neglected in the presented theory. We hope to address these issues in future work.

## 7 Conclusion

The relations between internal conformational dynamics of complex biomolecular systems and their ability to move directionally are of considerable interest in many fields. Ab initio simulation of coupled conformational and translational dynamics is usually of high computational cost and often not illuminating. In this paper we studied a reduced model where the internal dynamics of a motor is not considered explicitly but is assumed to result in periodic variation of the strength of the microscopic potential through which the motor interacts with molecules of the surrounding thermal bath. The model is simple enough to allow the evaluation of the driving force in an analytic form. In contrast to many models with variation of external parameters, our model shows no directional motion in adiabatic approximation of infinitely slow (reversible) variations. Moreover, the leading-order correction to the adiabatic approximation (linear in the variation frequency  $\omega$ ) is also insufficient: Without the last two terms quadratic in  $\omega$ , the Langevin equation (59), or (56), has a no-drift solution. Interestingly, those two terms, if only one of them is left in (59), generate the drift in opposite directions. Thus, being the interplay of two terms, the direction of motion of the motor can hardly be predicted with qualitative arguments.

The model can be extended in many ways. Since the role of internal variations is to drive the motor out of equilibrium, it is clear that a strictly periodic and deterministic character of variations is unnecessary to maintain the drift. One may expect a similar mechanism of directional transport, for instance, for motors driven by internal conformational transitions which, due to the fuel consumption, do not satisfy the equilibrium detailed balance condition. Models with stochastic transitions between two and more internal conformational states were discussed earlier [24], but they implied the existence of the external potential(s), whereas our motor is autonomous.

**Acknowledgements** I thank to G. Buck, G. Parodi, and J. Schnick for discussions, and to an anonymous referee for valuable comments.

## Appendix

This Appendix (not included in the published version) presents perturbation solutions of Eq. (41) to second order in the small parameter  $\epsilon = \omega\tau^0$ . The

equation has a form

$$1 + c_1 x + \epsilon c_2 x^2 + \epsilon^2 c_3 x^3 = 0$$

where  $x = \tau^*/\tau^0$  and

$$c_1 = -\xi(t), \quad c_2 = -\frac{a}{3} \cos \omega t, \quad c_3 = \frac{a}{12} \sin \omega t.$$

Substituting into the equation the second-order ansatz

$$x = x_0 + \epsilon x_1 + \epsilon^2 x_2$$

and discarding terms of order higher than two yields

$$1 + c_1(x_0 + \epsilon x_1 + \epsilon^2 x_2) + \epsilon c_2(x_0^2 + 2\epsilon x_0 x_1) + \epsilon^2 c_3 x_0^3 = 0.$$

Equating to zero contributions of each order separately

$$1 + c_1 x_0 = 0, \quad c_1 x_1 + c_2 x_0^2 = 0, \quad c_1 x_2 + 2 c_2 x_0 x_1 + c_3 x_0^3 = 0,$$

one finds

$$x_0 = -\frac{1}{c_1}, \quad x_1 = -\frac{c_2}{c_1^2}, \quad x_2 = \frac{c_3}{c_1^3} - \frac{2 c_2^2}{c_1^4}.$$

For  $\tau^* = x \tau^0$  these relations lead to the solution (42). One can show that two other solutions are singular (diverge as  $\epsilon \rightarrow 0$ ) and have no physical meaning.

## References

1. N. Van Kampen, *Stochastic Processes in Physics and Chemistry*, North-Holland, 2007, Chapter V.
2. B. Cleuren and C. Van den Broeck, *Granular Brownian motor*, Europhys. Lett. 77, 50003 (2007); J. Talbot, R. D. Wildman, and P. Viot, *Kinetics of a Frictional Granular Motor*, Phys. Rev. Lett. 107, 138001 (2011); A. Sarracino, A. Gnoli, and A. Puglisi, *Ratchet effect driven by Coulomb friction: The asymmetric Rayleigh piston*, Phys. Rev. E 87, 040101(R) (2013).
3. R. Golestanian, T. B. Liverpool, and A. Ajdari, *Propulsion of a molecular machine by asymmetric distribution of reaction products*, Phys. Rev. Lett. 94, 220801 (2005); G. Rückner and R. Kapral, *Chemically Powered Nanodimers*, Phys. Rev. Lett. 98, 150603 (2007); P. H. Colberg and R. Kapral, *Angstrom-scale chemically powered motors*, EPL 106 30004 (2014).
4. D. Abreu and U. Seifert, *Extracting work from a single heat bath through feedback*, EPL 94, 10001 (2011); D. Mandal and Ch. Jarzynski, *Work and information processing in a solvable model of Maxwell's demon*, PNAS 109, 11641 (2012); Z. Lu, D. Mandal, and Ch. Jarzynski, *Engineering Maxwell's demon*, Phys. Today 67, 60 (2014).
5. S. Sporer, Ch. Goll, and K. Mecke, *Motion by stopping: Rectifying Brownian motion of nonspherical particles*, Phys. Rev. E 78, 011917 (2008).
6. P. Reimann and P. Hänggi, *Introduction to the physics of Brownian motors*, Appl. Phys A 75, 169 (2002).
7. P. Reimann, *Brownian motors: noisy transport far from equilibrium*, Phys. Rep. 361, 57 (2002).

- 
8. P. Romanchuk, M. Bär, W. Ebeling, B. Lindner, and L. Schimank-Geier, *Active Particles: From Individual to Collective Stochastic Dynamics*, Eur. Phys. J. Special-Topics 202, 1 (2012).
  9. Ch. Gruber and J. Piasecki, *Stationary motion of the adiabatic piston*, Physica A 268, 412 (1999).
  10. E. Kestemont, C. Van den Broeck, and M. Malek Mansour, *The adiabatic piston: And yet it moves*, Europhys. Lett, 49, 143 (2000).
  11. T. Munakata and H. Ogawa, *Dynamical aspects of an adiabatic piston*, Phys. Rev. E 64, 036119 (2001)
  12. C. Van den Broeck, R. Kawai, and P. Meurs, *Microscopic analysis of a thermal Brownian motor*, Phys. Rev. Lett. 93, 090601 (2004).
  13. P. Meurs, C. Van den Broeck, and A. Garcia, *Rectification of thermal fluctuations in ideal gases*, Phys. Rev. E 70, 051109 (2004).
  14. P. Meurs and C. Van den Broeck, *Thermal Brownian motor*, J. Phys.: Condens. Matter 17, S3673 (2005).
  15. A. V. Plyukhin and A. M. Froese, *Nonlinear dissipation effect in Brownian relaxation*, Phys. Rev. E 76, 031121 (2007).
  16. A. V. Plyukhin and J. Schofield, *Langevin equation for the extended Rayleigh model with an asymmetric bath*, Phys. Rev. E 69, 021112 (2004).
  17. P. Reimann, R. Bartussek, R. Häussler, and P. Hänggi, *Brownian Motors Driven by Temperature Oscillations*, Phys. Lett. A 215, 26 (1996).
  18. S. von Gehlen, M. Evstigneev, and P. Reimann, *Ratchet effect of a dimer with broken friction symmetry in a symmetric potential*, Phys. Rev. E 79, 031114 (2009).
  19. J. M. R. Parrondo, *Reversible ratchets as Brownian particles in an adiabatically changing periodic potential*, Phys. Rev. E 57, 7297 (1998).
  20. R. D. Astumian, *Adiabatic operation of a molecular machine*, Proc. Natl. Acad. Sci. 104, 19715 (2007).
  21. S. Rahav, J. Horowitz, and Ch. Jarzynski, *Directed Flow in Nonadiabatic Stochastic Pumps*, Phys. Rev. Lett. 101, 140602 (2008).
  22. V. Y. Chernyak and N. A. Sinitsyn, *Pumping Restriction Theorem for Stochastic Networks*, Phys. Rev. Lett. 101, 160601 (2008).
  23. A. V. Plyukhin, *Brownian diode: Molecular motor based on a semi-permeable Brownian particle with internal potential drop*, Phys. Lett. A 377, 1037 (2013).
  24. J. Prost, J.-F. Chauwin, L. Peliti, A. Ajdari, *Asymmetric pumping of particles*, 72, 2652 (1994); F. Jülicher, A. Ajdari, J. Prost, *Modeling molecular motors*, Rev. Mod. Phys. 69, 1269 (1997); H. Hagan, M. Zelan, C. M. Dion, *Breaking the symmetry of a Brownian motor with symmetric potentials*, J. Phys. A 44 (15), 155002 (2011).